A Critical Analysis of Methods of Calculation of a Potential in Simulated Polar Liquids: Strong Arguments in Favor of "Molecule-Based" Summation and of Vacuum Boundary Conditions in Ewald Summation

Yury N. Vorobjev[†] and Jan Hermans*

Department of Biochemistry and Biophysics, University of North Carolina, Chapel Hill, North Carolina 27599-7260

Received: October 23, 1998; In Final Form: August 31, 1999

The calculation of the electrostatic potential inside a polar liquid in an infinitely large system simulated with periodic boundary conditions allows several alternative choices for carrying out the summation over all particles. For a summation of contributions from charge centers limited to the contents of a sphere surrounding the point where the potential is calculated, the cutoff can be based on the location of individual charge centers (so-called q-based summation) or on the location of molecular centers (M-based summation); these two methods have been found to provide consistently different values of the potential. On the other hand, for a summation based on the Ewald method, the choice of the latter's boundary conditions ("vacuum" versus "tinfoil") affects the value of the calculated potential. A recent discussion (see, Aqvist et al. *J. Phys. Chem.* **1998**, *B 102*, 3837−3840, and references therein) did not lead to a conclusion as to which is the right choice. Here, we provide a new analysis of M- and q-based cutoff methods and show the following. (i) The M-based method is the correct method to calculate the Coulombic average potential exerted by a polar molecular liquid in the center of a Lennard-Jones (LJ) solute. (ii) Each solute−solvent force field is characterized by a unique M-center for which the potential is zero in the high-temperature limit. This unique M-center is the center of the solvent−solute hard-core interaction for which the solvent molecule's orientational phase space is uncoupled from its positional phase space in the rotational high-temperature limit. (iii) The best value of the average Coulomb potential of water solvent inside a "methane" LJ solute in SPC water at $T = 300$ K and $P = 1$ bar is negative, of the order of -7 to -8 kcal/(mol·e); this includes a uniform potential of the order of $+2$ to $+3$ kcal/(mol·e) produced by the polarized surface of the outer liquid−vapor interface of a macroscopic droplet. (iv) The q-based method of calculation of the potential violates the self-consistency of statistical sampling of the configurations of charged sites of the solvent molecules. (v) The effective M- or q-based potentials calculated with Ewald "vacuum" potential are equal to the respective Coulombic potentials. (vi) Use of "tinfoil" boundary conditions for the Ewald potential overestimates the interaction of the central cell with its surroundings and enhances periodicity, and is therefore less appropriate for simulations of liquid systems.

1. Introduction

The calculation of the electrostatic potential inside a polar liquid in an infinitely large system simulated with periodic boundary conditions allows several alternative choices for carrying out the summation over all particles. On one hand, for a summation of contributions from charge centers limited to the contents of a sphere surrounding the point where the potential is calculated, the cutoff can be based on the location of individual charge centers (so-called q-based summation) or on the location of molecular centers (M-based summation). In other words, a simple cutoff method[1] can select the charged sites to be included charge-by-charge, or it can select molecular centers, and on that basis include or exclude all charged sites of the molecule at once. These two methods have been found to provide consistently different values of the potential. Of the two, the M-based (or group-based) cutoff method shows faster convergence with increasing cutoff distance, R_C, and is standard in many simulation methods.[16] On the other hand, for a summation based on the Ewald method no cutoff is used, but the choice of the Ewald boundary conditions ("vacuum" versus "tinfoil") affects the value of the calculated potential.

Calculation of the electrostatic potential in simulated water has been a subject of extensive recent controversial discussion.[3,4,12,13] The cited papers report calculations of the value of an average electrostatic potential induced by solvent water molecules at the center of an uncharged Lennard-Jones (LJ) particle, but fail to prove which is the right method, and, hence, what is the correct value of the potential. The results of these studies are summarized in the following paragraphs.

Rick and Berne[18] modeled recharging of a probe SPC water molecule, in molecular dynamics (MD) simulations with periodic boundary conditions (PBC), with use of Ewald summation, NTV ensemble, and standard conditions $T = 300$ K and density $= 1$ g/cm^3. Using the M-based method they found a negative potential $\langle\phi(0)\rangle = -10$ kcal/(mol·e) at the center of the uncharged probe (all three atomic partial charges set to zero).

Aqvist and Hansson[2] modeled the same problem by MD simulation of a spherical system of water molecules with an uncharged probe molecule at the center. The droplet had a radius

* Corresponding author e-mail: hermans@med.unc.edu. Telephone: (919) 966−4644.

[†] On leave from the Novosibirsk Institute of Bioorganic Chemistry, Novosibirsk, 630090, Russia. E-mail: vorobjev@femto.med.unc.edu. Telephone: (919) 966-8625, fax: (919) 966-2852.

10.1021/jp984211q CCC: $18.00
Published on Web 10/28/1999

of 15 Å maintained with a surface restraint potential and a cutoff of 10 Å in the force calculation. They found a negative value for the potential exerted at the center of the probe by the entire system, $\langle\phi(0)\rangle = -8.7$ kcal/(mol·e).

Hummer and Garcia[11] using Monte Carlo simulation with Ewald sum and tinfoil boundary conditions, showed that the value of the potential at the center of an LJ "methane" molecule calculated via the q-based method either with Coulombic (one-copy) or with ES (multicopy) effective tinfoil potential converge to the same value, $\langle\phi(0)\rangle \sim +10$ kcal/(mol·e).

Ashbaugh and Wood[5] found a value for the potential $\langle\phi(0)\rangle$ of ca. −10 kcal/(mol·e) using the M-based method with cutoff near 9 Å, and $\langle\phi(0)\rangle$ equal to ca. +10 kcal/(mol·e) using the Ewald method with tinfoil boundary conditions.

Despite these differences in $\langle\phi(0)\rangle$, the values of the polarization free energies for charging the probe water molecule obtained in several studies[2,10,18,] with different methods are in a good agreement; i.e., Rick and Berne,[18] with PBC and Ewald summation with vacuum boundary conditions, obtain a value of −8.4 kcal/mol, Aqvist and Hansson,[2] modeling a finite spherical system, obtain −8.6 kcal/mol, and Hummer and Garcia,[11] using PBC and Ewald summation with tin-foil boundary conditions and a self-energy term, find −8.50 kcal/mol.

Hummer et al.[12] have calculated the potential $\langle\phi(0)\rangle$ by both M- and q-based methods for the results of MC simulations of finite water clusters and for an infinite system simulated with PBC and Ewald summation. The results of these calculations (see Figure 2 of ref 12) show that for finite clusters of 256 or 1024 molecules, the M-based and q-based potentials converge to similar values of ca. −6 to −7 kcal/(mol·e). On the other hand, for an infinite system with PBC, the M-, and q-based potentials converge to different values, of about −10 and +10 kcal/(mol·e), respectively. Furthermore, the M-based potential converges to a different value with a different choice of the M-center (oxygen atom or midpoint of the two hydrogen atoms). The choice of boundary condition in the Ewald method also affects the value of the potential. At the same time, several studies[5,18] and also our simulations lead to the conclusion that water configurations around an uncharged LJ solute are indistinguishable, whether obtained in simulations with cutoff in the range of 10 to 12 Å or with use of Ewald summation for long-range electrostatic interactions.

Hummer et al.[11] justify finding a positive potential with the argument "the asymmetry of the charge distribution on the water molecule gives rise to a positive potential that is primarily caused by the hydrogens penetrating the LJ sphere of the methane particle." This explanation is unsatisfactory, because all of the authors cited above found similar water structure around the LJ solute with water dipoles having a distinct preference to point their negative dipole end toward the solute.[2,11,12,18] (The TIP4P water also shows preferred direction of the negative dipole side to the LJ solute.[14]) Hummer et al.[12] also conclude that the M-based calculation of the potential $\langle\varphi\rangle$ corresponds to unphysical behavior. We do not challenge the numerical results of Hummer's calculations,[12] but we do not support the cited conclusion about unphysical behavior of the M-based potential.

This paper presents an analysis of the q-, and M-based potentials and the M-center dependence of the potential $\langle\phi_{M}(0)\rangle$. Relevant aspects noted earlier by others have been included explicitly in order to create a comprehensive basis for analysis. We conclude that for a given solute−solvent force field a unique M-center exists which should be used for the M-based method of calculation, and that M-based summation with use of this unique M-center produces the physically correct value of the electrostatic potential in a polar liquid. This unique M-center (M_h-center) is the center of the solvent−solute interaction for which the solvent molecule orientational phase space is uncoupled from its positional phase space. For the M_h-center, the rotational high-temperature limit of the potential is zero. Use of the M-based method with other choice of the M-center produces a residual artificial cutoff surface potential. The q-based method violates the statistical self-consistency of sampling of solvent configurations contributing to the average value of the electrostatic potential.

Finally, we find that effective M-, or q-based potentials calculated with Ewald (i.e., multicopy) summation using "vacuum" boundary conditions are equal to the respective Coulombic (i.e., single copy) potentials, whereas use of tinfoil boundary conditions for the Ewald potential enhances periodicity and appear to be less appropriate for simulations of what are ultimately macroscopically finite systems.

2. Rotational High-Temperature Limit of the M-Based Potential

In this section we develop the idea that in a high-temperature limit, which we define as a temperature sufficiently high that the rotational correlation of all solvent molecules, including those around the LJ solute and at the outer surface of a liquid drop is negligible, the real physical electrostatic potential exerted by the solvent should be zero. Specifically, this is a limit where the intermolecular electrostatic energies are insufficient to preferentially orient the molecules, but a repulsive intermolecular potential persists to keep the molecules separated from each other, acting very much like a repulsive core potential in a liquid of isotropic molecules.

A simulation potential depends on the sampling of the charged sites of solvent molecules positions and orientations. A molecule's position can be defined in terms of an M-center, $\mathbf{r_{i,M}}$ which is often the center of mass, and its orientation in terms of three angles Ω_i.[8] The full configurational space Γ in a pure molecular liquid is the product of the rotational Ω_i and translational $\mathbf{r_{i,M}}$ subspaces for any center M, i.e., $\Gamma = \{\mathbf{R}\}_\mathbf{M} \cdot \{\Omega\}_\mathbf{M}$. If a molecule's rotational probability distribution is uniform (in some position), then the rotational average of the potential produced by molecules (in this position) is zero. One can see that this must be so, because a rotated polar molecule can be presented as a rotation image, i.e., a set of concentric charged spheres with radii h_α and surface charge density which depends on the solvent orientational distribution. For a uniformly rotated solvent molecule, the surface charge density is uniform (equal to $q_\alpha/4\pi h_\alpha^2$) for each charged molecular site α, where h_α is the distance from the center of molecular rotation to the charged atomic site α. According to elementary electrostatics, a collection of concentric spherical charged surfaces with net charge zero produces zero Coulombic potential outside the largest sphere.[15] However, a nonuniform orientational distribution of solvent molecules makes the surface charge density of these spheres nonuniform, and this will result in some finite value of the potential.

The $\mathbf{R_M}$ and $\Omega_\mathbf{M}$ spaces are restricted by the solute−solvent repulsive interaction and physical outer surface of the solvent drop; furthermore, they are in general not independent, i.e., the rotational domain $\Omega_\mathbf{M}(\mathbf{r_{i,M}})$ of a solvent molecule is not a full rotation but it is a function of the position $\mathbf{r_{i,M}}$ and also of the choice of the M-center. For a given solvent molecule (in the high-temperature limit) there is a unique M_h-center for which $\mathbf{R_M}$ is restricted but the rotational space $\Omega_\mathbf{M}$ is either not

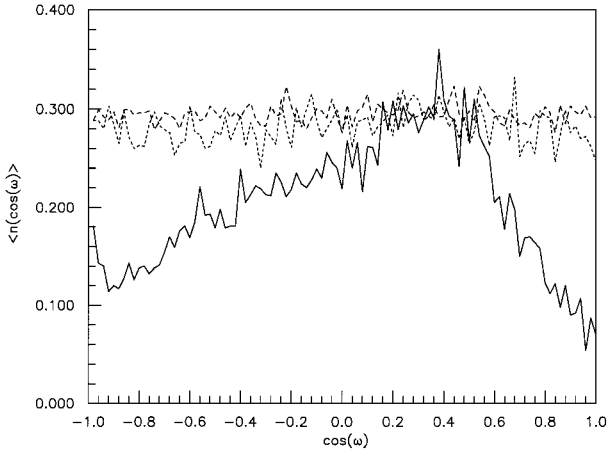

Figure 1. Orientational correlation function $\langle n(\cos\omega)\rangle$, for water molecules in the first (solid line), second (short dashed line), and third (long dashed line) hydration shells of an LJ "methane" molecule, obtained via MD simulations at $T = 300$ K, $P = 1$ bar with PBC for 1000 configurations along a 250 ps equilibrium trajectory.

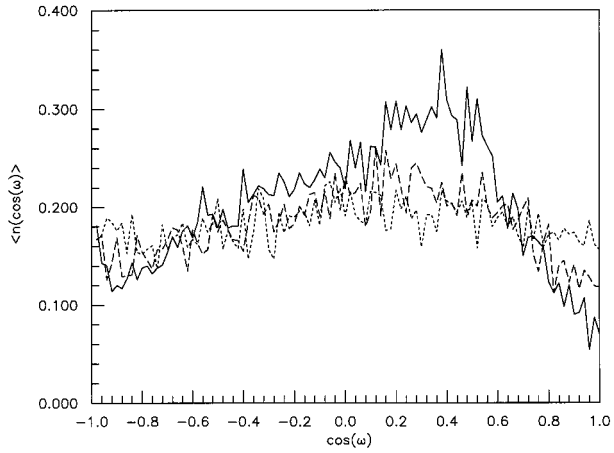

Figure 2. Orientational correlation function $\langle n(\cos\omega)\rangle$ for water molecules in the first hydration shell of an LJ "methane" molecule, obtained via MD simulations at $T = 300$, 500, and 1000 K (solid, long dashed, and short dashed lines, respectively).

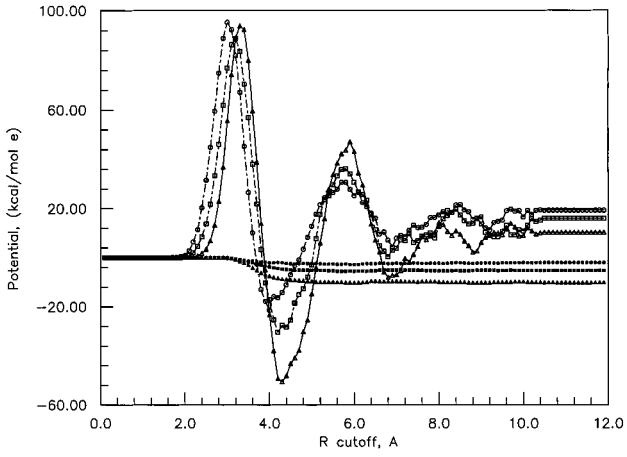

Figure 3. The M-based $\langle\phi_M(0; R_C)\rangle$, and q-based $\langle\phi_q(0; R_C)\rangle$ potentials of water solvent in the center of an LJ "methane" molecule, calculated from 250 ps MD simulations at three different temperatures. M-based potential: ▲, ■, ●; q-based potential: △, □, ○ for $T = 300$, 500, 1000 K, respectively.

restricted (uncoupled), or at least optimally isotropic for each accessible position of the M_h-center. For the SPC, TIP3P, and TIP4P water models the oxygen atom alone acts as a center for short-range repulsive interactions, and for these models the M_h-center coincides with the position of the oxygen atom, the usual choice of M-center for these models. Other proposed choices of molecular center of, respectively, the dipole midpoint[3] and the center of mass[8] do not correspond to the interaction center M_h for which the rotational orientation is isotropic. In a rotational high-temperature limit when solute−solvent orientation correlations are negligible, the M-based potential for the M_h-center has zero value. It should be noted that at high temperature the potential is zero, independent of the solvent−solute (distance) pair correlation function. When the solution cools, solvent−solute orientation correlations emerge and the potential $\langle\phi_{Mh}(0, R_C)\rangle$ will gain some nonzero value from the first solvation shell, etc.

Results of MD simulations of an LJ "methane" molecule in SPC water solution with PBC in a cubic box of edge 12 Å, with cutoff distance 11.5 Å, at temperatures of 300 K (NTP ensemble, $P = 1$ bar), 500 and 1000 K, (NTV ensemble), confirm the above conclusions. Figure 1 shows the solvent−solute orientation correlation as the distribution $\langle n(\cos\omega)\rangle$ for water molecules in the first, second, and third hydration shells, where ω is the angle between a water molecule's dipole μ and the vector connecting the center of the solute molecule to the center of the probe molecule. For a temperature of 300 K, the solvent−solute orientation correlation is marked for the first hydration shell, a maximum of the function $\langle n(\cos\omega)\rangle$ at $\cos\omega$ ca. 0.4 showing a preferable orientation of the negative end of the water dipoles toward the solute cavity. For the second and third hydration shells the orientation correlations are negligible. Figure 2 shows that the solvent−solute orientation correlation in the first hydration shell decreases with an increase of the solution temperature. Finally, Figure 3 shows that the decrease of the solvent−solute orientation correlations at higher temperature results in decrease of the M_h-center-based electrostatic potential, with converged values (at high R_C) equal to −10, −5, −2 kcal/(mol·e) at temperatures of 300, 500, and 1000 K, respectively. Figure 3 also shows that the M_h-based potential is essentially converged when the cutoff distance R_C exceeds 7 Å, i.e., when it includes the second hydration shell (cf. also Hummer et al.[12]). Extrapolating this to a limit of very high temperature, in which the solvent molecules are excluded from the central cavity (the LJ solute) and restricted to lie within an outer surface, but their orientations are not restricted, the M_h-based potential will be identically equal to zero for all values of R_C, while this will not be true of the q-based potential and of other choices of the M-center (cf. also Hummer et al.[12]).

3. Origin of the Difference between M- and q-Based Potentials

A difference in potential $\langle\delta\phi(0;R_C)\rangle$ between M-based and q-based potentials

$$\langle\delta\phi(0;R_C)\rangle = \langle\phi_M(0;R_C)\rangle - \langle\phi_q(0;R_C)\rangle \qquad (1)$$

can be calculated analytically under the reasonable assumption that at large distance r from the LJ solute and the outer drop surface (i) the average distribution of M-centers is uniform, with density equal to that of the solvent, ρ_w, and (ii) the rotational distribution of solvent molecules around their M-centers is random and independent of the choice of the M-center.

This potential difference corresponds to a difference between the charge densities which contribute to the q-, and M-based potentials $\langle\delta Q(r)\rangle = \langle Q_M(r) - Q_q(r)\rangle$. This difference in charge density is nonzero only in the vicinity of the cutoff sphere R_C. If the M-center is inside the cutoff sphere, then a portion of the

spherical surface on which a particular charge center q_α may lie will be outside the cutoff sphere and will contribute to the M-based potential, whereas it will not contribute to the q-based potential, and this gives a charge density deficit. Similarly, if the molecular center is outside the cutoff sphere**,** then this position does not contribute to the M-based potential, but a portion of the charge distribution for each charge center penetrates inside the cutoff sphere contributing to the q-based potential and giving an excess charge density. As has been discussed in a number of papers,[2−5,13,21] the magnitude of this potential is a function of the molecular geometry and the choice of M-center, independent of the value of the cutoff radius, and is given by

$$\langle \delta\phi(0)\rangle = -\frac{2\pi\rho_w}{3}\sum_\alpha q_\alpha h_\alpha^2 \qquad (2)$$

the summation being over all charge centers, and h_α the distance of a particular charge center from the M-center. The result is also independent of temperature, the assumption being that the cutoff surface is enough distant from perturbing surfaces (the surface of the LJ probe and any outer surface of the sample), that the orientational distribution of the molecules is uniform. The charge density $\langle Q_q(r)\rangle$ is obviously equal to zero under assumption of uniformity of rotational and positional distribution of the solvent molecules at the cutoff sphere R_C , therefore the potential $\langle \delta\phi(0)\rangle$ is generated by the charge density $\langle Q_M(r)\rangle$ at the cutoff sphere R_C.

For the SPC water model with M-center at the oxygen atom, the potential $\langle \delta\phi\ (0;\ M = O)\rangle$ estimated from eq 2 is equal to −18.99, while with a choice of M-center at the midpoint between the two H-atoms $\langle \delta\phi(0;\ M = HH)\rangle = -6.3$ kcal/(mol·e). For estimates of these potentials obtained by Hummer et al. for sample configurations from Monte Carlo simulation, given in Figure 2 of that work,[12] the difference $\langle \delta\phi(0)\rangle$ is close to −18 and −6 kcal/(mol·e) for M = O and M = HH, respectively. This is true both for results obtained in an infinite water solvent with PBC, or in finite clusters for R_C around 7 or 8 Å. Our calculations of the potentials $\langle \phi_q(0;\ R_C)\rangle$ and $\langle \phi_M(0;\ R_C)\rangle$ for samples generated by molecular dynamics simulation show a difference $\langle \delta\phi(0)\rangle$ of around −20 kcal/mol, independent of temperature (T = 300, 500, 1000 K; cf. Figure 3). These simulated results are in good agreement with the analytical result derived here. Our MD simulations (results not shown here) demonstrate also that the potentials $\langle \phi_q(0;\ R_C)\rangle$ and $\langle \phi_M(0;\ R_C)\rangle$ are almost independent of the method of treatment of the long-range forces in our MD simulations, i.e., with a cutoff of 11.5 Å or with long-range forces included with use of Ewald summation.

The above simple treatment shows that the difference potential $\langle \delta\phi(0)\rangle$ generated by a difference in charge density $\langle \delta Q(r)\rangle$ can be attributed to the partial inclusion in q-based sampling of molecules that are intersected by the cutoff surface. Neglect of some portion of a molecule, $M_{i\beta}$ while including another portion, $M_{i\alpha}$ physically means that the correlation between the probabilities of including the centers in the sampling, $\langle P(M_{i\alpha})P(M_{i\beta})\rangle$, is zero, while this internal correlation function is in fact always equal to unity. Thus, q-based sampling with finite cutoff violates intramolecular site−site correlation and produces a sampling that is statistically not self-consistent.

4. Solvent Charge and Dipole Densities

To further analyze the difference between M- and q-based methods we consider the charge densities near physical surfaces and near a computational cutoff surface. These are estimated from simulations and also analytically in a rotational high-temperature limit. We consider specifically the charge densities $\langle Q(r;\ R_C)\rangle$ as a function of radial distance, r, in calculations with cutoff R_C, that result from application of the q-based and M-based cutoff methods. These are unequal only when the difference between r and R_C is less than the size of a solvent molecule. It is shown that the charge density has a dipole density term at the surface of an LJ solute placed at the center (inner or cavity surface), and again at the outer surface of a finite system (i.e., a water drop), which does not vanish in the high-temperature limit. The charge density $\langle Q^M(r)\rangle$ has a dipole term at the surface of the cutoff sphere R_C, whose contribution to the electrostatic potential at the center exactly equals that produced by the dipole density at the water drop outer surface and exactly cancels that produced by the dipole density at the inner surface, if and only if the M-center is equivalent to the M_h-center. While for other choices of the M-center and for the q-based method the cancelation is not exact because of the specific sampling of solvent molecules. At finite temperature, physical interactions produce additional solvent polarization near the surface of the LJ solute and near the surface of the droplet.

The following derivation assumes a rotational high-temperature limit, in which the centers of solvent molecules are restricted to the volume between the surface of the LJ particle (inner surface, radius R_{LJ}) and the outer surface of the drop (radius R_D), with a uniform orientation. Charged atoms (charge q_α at distance h_α from the molecular center) can occur in a slightly larger volume, namely, at positions $R_{LJ} - h_\alpha < r_\alpha < R_D + h_\alpha$, with $R_{LJ} > h_\alpha$. This generates an uneven charge distribution near the surface; for example, for SPC water, some hydrogen atoms will be found in a thin layer outside the surface, which will have a positive charge density, compensated by a negative charge density elsewhere.

The charge density may be found by considering the contribution generated by the rotational image of a single charge q_α for every possible position of the M-center, and summing over all charge centers, following the same derivation as was used to obtain the potential difference for use of M- and q-based cutoffs, eq 2.[2−5,13,21] In the rotational high-temperature limit the orientational distribution of the solvent is uniform, and the charge density depends only on the distribution of molecular centers, $\rho_w g_M(r)$, if the positional $\{\mathbf{R}\}_\mathbf{M}$ and rotational subspaces $\{\Omega\}_\mathbf{M}$ are uncoupled as it is defined for the M_h-center. The radial charge density contributed by a single charge center is given by

$$\langle Q_\alpha(r)\rangle = \frac{\rho_w q_\alpha}{2rh_\alpha}\int_{r-h_\alpha}^{r+h_\alpha} r_M g_M(r_M)\mathrm{d}r_M \qquad (3)$$

with the total charge density given by

$$\langle Q(r)\rangle = \sum_\alpha \langle Q_\alpha(r)\rangle \qquad (4)$$

It is easy to see that the charge density is equal to zero except where $g_M(r)$ varies with distance, which is only true close to either surface. The total charge density can therefore be written as the sum of the charge densities for regions near the inner surface (r near R_{LJ}) and the outer surface (r near R_D)

$$\langle Q(r)\rangle = Q_{inner}(r;\ R_{LJ}) + Q_{outer}(r;\ R_D) \qquad (5)$$

The total potential $\varphi(0)$ of a solvent drop at the solute center is equal

$$\varphi(0) = 4\pi\rho_w\int_0^\infty \langle Q(r; R_D)\rangle\, r\mathrm{d}r$$

$$= 4\pi\rho_w\sum_\alpha \frac{q_\alpha}{h_\alpha}\{\int_0^{h_\alpha} r^2 g_M(r; R_D)\mathrm{d}r + h_\alpha\int_{h_\alpha}^{h_\alpha(\max)} r g_M(r; R_D)\mathrm{d}r\} \quad (6)$$

It can be seen that $\varphi(0) = 0$ if $g_M(r) = 0$ for $r < h_\alpha(\max)$ as it is for the LJ solvent with hard core. The inner surface (cavity) and outer surface charge densities each generate a potential at the center of the LJ solute. One can obtain the potential generated by the outer surface the same answer as in eq 2

$$\phi_{outer}(0) = 4\pi\rho_w\int_{R_O}^\infty Q_{outer}(r) r\mathrm{d}r = -\frac{2\pi\rho_w}{3}\sum_\alpha q_\alpha h_\alpha^2(M_h) \quad (7)$$

where R_O is a large distance for which $g_M(R_O) = 1$. Respectively, the inner surface potential

$$\phi_{inner}(0) = \varphi(0) - \phi_{outer}(0) = \varphi(0) + \frac{2}{3}\pi\rho_w\sum_\alpha q_\alpha h_\alpha^2(M_h) \quad (8)$$

thereby, the inner and outer surface potentials cancel each other. It should be pointed out that the last expressions are valid if the M-center is the M_h-center.

For the SPC water model the values of the potentials (inner/outer) are $\pm$18.99 (kcal/mol·e). The surface charge densities at the inner and outer surfaces correspond to a density of surface dipoles, μ_s, pointed radially outward

$$\mu_s = \mp\frac{\rho_w}{6}\sum_\alpha q_\alpha h_\alpha^2 \quad (9)$$

(Cf. the rule, which follows from Gauss' theorem,[15] that a closed surface with uniform surface dipole density produces a uniform potential in the volume enclosed by the surface

$$\phi_{sdip} = -4\pi\mu_s \quad (10)$$

which is independent of size and shape of the surface.)

The point of deriving these results is that these allow one to assess the effect of (artificially) applying a distance cutoff to select which charges contribute to the potential at the center in samples produced in simulations. The cutoff surface (radius R_C) is at some distance from both inner and outer surfaces, where the distribution of charge and molecular centers is uniform. The cutoff effectively produces the following modified radial distribution function for M-centers

$$g_M(r; R_C) = g_M(r)\ r < R_C$$
$$= 0\ r > R_C \quad (11)$$

If the cutoff is based on the distance to the center of individual charges (q-based), then no net (average) charge density is produced near the cutoff surface. However, if the cutoff is based on molecular centers, a dipole charge density at the cutoff surface at radius R_C will be produced of a similar form as is produced by a physical outer surface, i.e.,

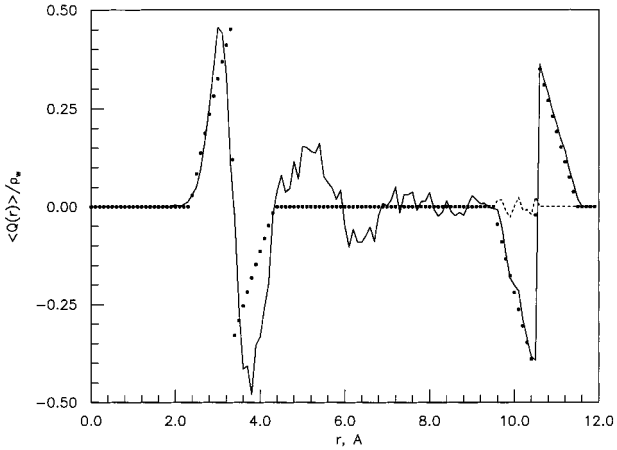

Figure 4. The radial charge densities $\langle Q^M(r; R_C)\rangle$, $\langle Q^q(r; R_C)\rangle$ normalized to a water density $\rho_w = 1$. Results based on MD simulations at $T = 300$ K, $P = 1$ bar, for $R_C = 10.5$ Å are represented by a solid line (M-based method) and by a dashed line (q-based method, where this does not coincide with the solid line). The rotational high-temperature limit of the M-based charge density with $R_{LJ} = 3.35$ Å is also indicated (dots).

$$Q^M(r; R_C) = Q_{inner}(r; R_{LJ}) + Q_{outer}(r; R_C)$$
$$Q^q(r; R_C) = Q_{inner}(r; R_{LJ})\ R_C < R_D \quad (12)$$

and ditto for the surface potential inside the surface generated by the corresponding surface dipole density. In other words, the M-based method of calculation generates a potential by the surface charge density $Q_{outer}(r; R_C)$ at the cutoff surface R_C which is defined by eq 7 for any M-center in simulations. The total potential $\varphi_M(0)$ generated by charge densities of the inner $Q_{inner}(r; R_L)$ and the cutoff surfaces $Q_{outer}(r; R_C)$

$$\varphi_M(0) = \frac{2}{3}\pi\rho_w\sum_\alpha q_\alpha[h_\alpha^2(M_h) - h_\alpha^2(M)] \quad (13)$$

Thereby, the cutoff surface potential, eq 2, exactly mimics the potential generated at the outer surface of a macroscopic water drop, eq 7, if the simulation M-center is equal to the M_h-center, and cancels the potential generated by the inner surface. The q-based method ignores the potential generated by the outer surface. Consequently, the potential calculated with a (microscopic) cutoff based on M_h centers is equal to the potential generated by the whole (microscopic or macroscopic) solvent drop (in the assumption of random orientation of solvent molecules at the outer surface). (Of course, if the cutoff distance contains an entire water drop, i.e., if $R_C > R_D$, the q- and M-based charge densities are equivalent.)

Figure 4 shows the rotational high-temperature limit of the charge densities for a cutoff distance R_C of 10.5 Å; filled circles represent $\langle Q^M(r; R_C)\rangle$ and open circles represent $\langle Q^q(r; R_C)\rangle$ where this has a different value (for values of r near R_C). Positive and negative excess charge density occurs first near the surface of the probe, and again in the neighborhood of the cutoff surface. The charge density near the cutoff surface depends on the method of computation, the M-based charge density having a large apparent surface term, while the q-based charge density remains close to zero. Figure 4 shows also the charge densities calculated from samples obtained with MD simulations with periodic boundary conditions at $T = 300$ K, $P = 1$ bar (solid curve). The charge densities from MD simulations agree well

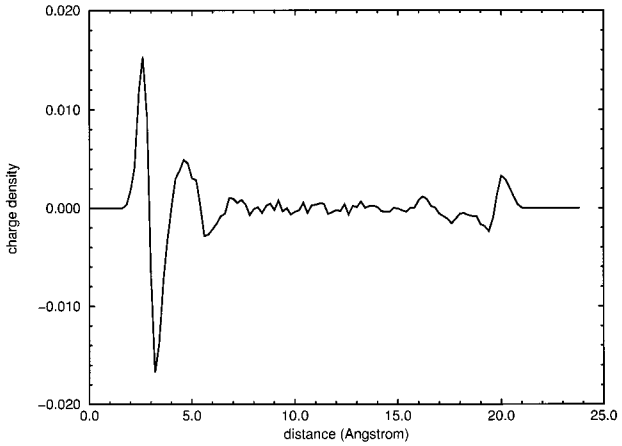

Figure 5. The charge density from simulations at 300 K of a droplet containing an LJ "water" particle at the center.

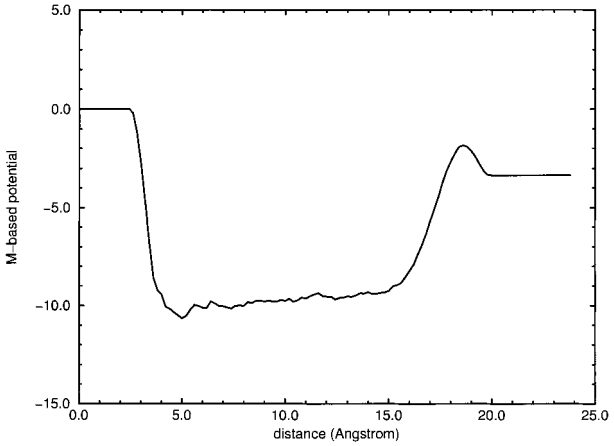

Figure 6. The M-based potential calculated at the center of the LJ particle, as a function of the cutoff distance R_C from these simulations.

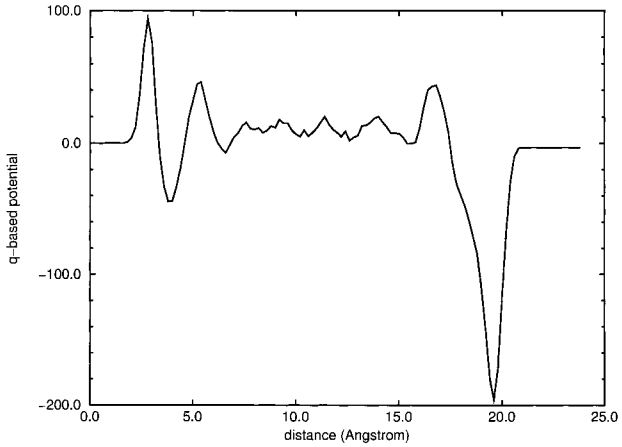

Figure 7. The q-based potential calculated at the center of the LJ particle, as a function of the cutoff distance R_C from these simulations.

with the theoretical estimation for the rotational high-temperature limit in the vicinity of the cutoff; on the other hand, deviations near the surface of the LJ solute indicate some preferential orientation of the water molecules. The related potentials from the MD simulations are shown in Figure 3.

Figures 5−7 show the charge density and M-based and q-based potentials at the center of a water droplet containing an LJ "water", simulated at 300 K. The charge density shows up−down spikes for the first and second coordination spheres (3 and 5 Å) and at the surface (19 Å). A net negative potential of ca. −10 kcal/(mol·e) is generated by M-based summation

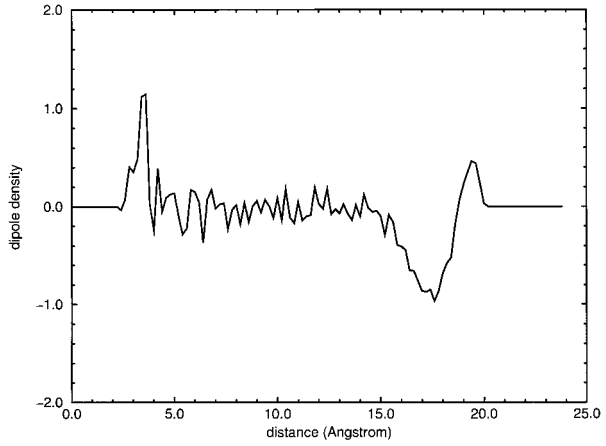

Figure 8. The radial component of the dipole density from simulations at 300 K of a droplet containing an LJ "water" particle at the center.

over the first shell, which is largely canceled when the summation includes also the polarized surface of the droplet. The q-based potential varies much more wildly, to reach a positive intermediate value of ca. +10 kcal/(mol·e), until inclusion of the surface layer produces a final net negative potential, which is (of course) equal to that found with M-based summation for large R_C. In the rotational high-temperature limit, the M-based summation gives a potential which is zero at all values of R_C, while q-based summation would produce a positive value of around 20 kcal/(mol·e) for intermediate cutoffs within the droplet's volume, Figure 3. One concludes that the M-based method of calculating the electrostatic potential in effect includes the rotational high-temperature limit of the potential produced by the charge distribution at the outer surface of a droplet, while the q-based method does not.

Hummer et al. have considered a different high-temperature limit, in which the molecules, including the solute probe, are in an ideal gas state, i.e., are both positionally and rotationally independent of one another.[13] They postulate that the potential at the center of the probe molecule is zero, and that this value is reproduced by q-based summation at any value of R_C, whereas M-based summation produces a nonzero potential at any value of R_C, given by eq 2. This has been taken as conclusive evidence in favor of the q-based summation method.[13] However, the postulate requires an infinite system, which, besides being unphysical, is not realizable in simulations, except if long-range interactions are (incorrectly) ignored. Even when long-range interactions are included with Ewald summation, treatment of an outer surface has to be specified (see below, section 5). Introduction of a surface requires specification of a radial density distribution near the surface which is equal to zero beyond some macroscopic distance from the center. As we have shown above, the surface then acts as a molecule-based cutoff and produces a potential inside the liquid. Accordingly, it is found that the M-based summation method, (assuming $g_M(r) = 1$ in eq 11) gives the correct answer also in this high-temperature limit.

At finite temperature a solvent molecule in the vicinity of an interface (i.e., near the surface of the LJ particle and near the outer surface of the droplet) has a preferable orientation, i.e., a surface polarization, which is not included in the above high-temperature limits of the charge densities. As can be seen from the mean radial component of the dipole moment, $\langle \mu_r \rangle$,

$$\mu_r = -q_O[(\mathbf{r}_{H_1} + \mathbf{r}_{H_2})/2 - \mathbf{r}_O)]\cdot\mathbf{r}_O/\mathbf{r}_O \qquad (14)$$

computed from simulation of a water droplet at 300 K (Figure 8), both inner and outer surfaces are polarized; at both surfaces

the water molecules prefer to orient their negative ends toward the surface. The polarization at the solute−solvent interface produces a potential at the center of the LJ solute of ca. −10 kcal/(mol·e), cf. Figures 3 and 6, while the polarization at the outer surface gives a positive contribution of 6.5 kcal/(mol·e), cf. Figure 6; the potential can be attributed largely to orientation of the water dipoles. Simulations have previously shown similar polarization at the surface of water droplets[6] and at planar interfaces between simulated water and vacuum.[17,19] One can expect the polarization of the outer surface of a macroscopic water droplet to become similar to that at a planar liquid−vapor interface as the radius R_D is increased. The surface polarization potential produced by the outer surface dipole density then approaches a constant value of $-4\pi\mu_s$ inside the water droplet, cf. eq 10. From simulations of SPC/E water, Taylor et al.[19] have found that the orientational distribution of water dipoles at the liquid−vapor interface produces surface polarization potentials of 7.6, 2.3, and 0.0 kcal/(mol·e) for $T = 268$, 298, and 373 K, respectively. Our result of 6.5 kcal/(mol·e) for a droplet in a hydrophobic cavity at 300 K indicates that the spherical boundary produces a stronger orientational polarization of water dipoles than does a planar liquid−vapor interface. The analysis suggests that the value of the potential at the center of an LJ "water" solute in a macroscopically finite SPC water drop is between −7 and −8 kcal/(mol·e) at $T = 300$ K, $P = 1$ bar.

5. Ewald Lattice Sum Potential

Monte Carlo and MD simulations of polar liquids with PBC may be considered as simulations in the usual minimum image convention but with the electrostatic part of the Hamiltonian[7] rewritten to include the contributions of all surrounding replica cells

$$H_{el} = \frac{1}{2}\sum_{\mathbf{n}}{}' \left[\sum_{i=1}^{N}\sum_{j=1}^{N} \frac{q_i q_j}{|\mathbf{r}_{ij} + L\mathbf{n}|} \right] \tag{15a}$$

where the first sum includes all simple cubic lattice points with integer coordinates (l, m, n), the prime indicates that terms with $i = j$ are omitted for $\mathbf{n} = 0$, and L is the edge of the simulation cube. To mimic a macroscopic solute droplet, the summation over $\mathbf{n} = (l, m, n)$ can be done for an infinite series of spherical shells and the electrostatic Hamiltonian can be presented as a sum of effective Ewald potentials $\phi_{EW}(r)$ between particles in the central cell with minimum image convention

$$H_{el} = \frac{1}{2L}\sum_{i\neq j}^{N} q_i q_j \phi_{EW}(\mathbf{r}_{ij}/L) + \frac{\xi}{2L}\sum_{i=1}^{N} q_i^2 \tag{15b}$$

Here $\phi_{EW}(r)$ is the Ewald potential[7] for an infinite lattice surrounded by a vacuum (vacuum boundary conditions) and replaces the Coulombic ($1/r$) potential so as to take into account of long-range electrostatic interactions all images of the charge q_j. If charge neutrality holds, (i.e., $\sum_{i=1}^{N} q_i = 0$), the "vacuum" Ewald potential is given by the following equation[7]

$$\phi_{EW}(\mathbf{r}/L) = \sum_{\mathbf{n}} \frac{erf(\eta|\mathbf{r}/L + \mathbf{n}|)}{|\mathbf{r}/L + \mathbf{n}|} + \frac{1}{\pi}\sum_{\mathbf{n}\neq 0} \frac{\exp(2\pi i \mathbf{n}\mathbf{r}/L - \pi^2|\mathbf{n}|^2/\eta^2)}{|\mathbf{n}|^2} - \frac{2\pi}{3}(\mathbf{r}/L)^2 \tag{16a}$$

The second term in eq 15b represents the self-energy of the charge in the central cell interacting with an infinite lattice of charge images on a uniform neutralizing background;[11] the parameter η is adjusted to minimize the computational effort needed to attain a given precision with truncated summations, and the value of the constant ξ is given by

$$\xi = \lim_{|r|\to 0}\left(\phi_{EW}(r) - \frac{1}{r}\right) = -2.837297 \tag{16b}$$

for a cubic lattice.

If the infinite spherical sample of cubic cells is surrounded by a conductor (tinfoil boundary condition) instead of by a vacuum, then the Hamiltonian includes additional reaction field terms;[7] the reaction free energy (per cell) of a spherical sample of radius R_{sample} of n cells is

$$H_{rf}^{tf} = -\frac{1}{n}\frac{(n|M|)^2}{2R_{sample}^3} = -\frac{2\pi|M|^2}{3L^3} \tag{17a}$$

where, $R_{sample}^3 = 3/4\pi nL^3$. Using the equality for the dipole moment M of an electrically neutral simulation box

$$|M|^2 = \sum_{i,j} q_i q_j r_i r_j = -\frac{1}{2}\sum_{i,j} q_i q_j r_{ij}^2 \tag{17b}$$

the tinfoil Hamiltonian can be written in the same form as eq 15b, but with tinfoil Ewald potential $\phi_{EW}^{tf}(r)$, which is related to the vacuum Ewald potential $\phi_{EW}(r)$ by[7]

$$\phi_{EW}^{tf}(r/L) = \phi_{EW}(r/L) + \frac{2\pi}{3L^3}r^2 \tag{17c}$$

The reaction field term in the tinfoil Ewald potential exactly cancels the last term in the expression for the vacuum Ewald potential given in eq 16a; therefore, the tinfoil Ewald potential is truly periodic in the cubic lattice.

Let us consider the M- and q-based potentials at the center of an LJ particle placed at the origin, calculated on the basis of Ewald potentials with the two different kinds of boundary conditions instead of Coulombic potential. Calculation with Ewald vacuum potential is equivalent to summation of Coulombic potentials from all images of the central cell. Consider first the case that the cutoff is a spherical surface with radius less than half the cell edge, $R_C < L/2$. With the reasonable approximation that the charge distribution inside the cutoff sphere has rotational symmetry, it follows that the images make no contribution to the potential at the center of the central cell. Therefore, one can conclude that as long as $R_C < L/2$, the q- and M-based potentials calculated with effective Ewald vacuum potential are equal to the respective potentials calculated with Coulombic potential

$$\langle\phi_{EW,q}(0; R_C)\rangle = \langle\phi_{C,q}(0; R_C)\rangle \tag{18a}$$

$$\langle\phi_{EW,M}(0; R_C)\rangle = \langle\phi_{C,M}(0; R_C)\rangle \tag{18b}$$

Results obtained by Hummer with MC simulation, cf. Figures 2 and 3 of reference 12 confirm this conclusion.

If the potential on the solute is calculated with the tinfoil potential $\phi_{EW}^{tf}(r)$, we then need to consider only the difference between the Ewald tinfoil and vacuum potentials, which is given by eq 17c

$$\phi_2(r) = \frac{2\pi r^2}{3L^3} \tag{19}$$

This term affects the total potential calculated by the M- and q-based methods, each in a different way.

Consider first the M-based distribution, an analytical expression for the integrated potential $\phi_2(0)$, i.e., at the center of the LJ solute. This can be obtained for the usual assumption of a uniform molecular orientation and distribution of molecular centers between the surface of the probe (at radius R_{LJ}) and the cutoff surface (at radius R_C) by treating each molecule as its rotational image

$$\langle\phi_{2,M}(0; R_C)\rangle = \rho_w \sum_\alpha \left(\frac{2\pi q_\alpha}{3L^3}\right) \int_{R_{LJ}}^{R_C} 4\pi r^2 dr \frac{1}{4\pi h_\alpha^2} \int_0^\pi (r^2 + h_\alpha^2 - 2rh_\alpha \cos\theta) 2\pi h_\alpha \sin\theta \, d\theta \quad (20)$$

and integration gives

$$\langle\phi_{2,M}(0; R_C)\rangle = \frac{8\pi^2\rho_M}{9}\left(\frac{R_C^3 - R_{LJ}^3}{L^3}\right)\sum_\alpha q_\alpha h_\alpha^2 \quad (21)$$

This potential depends strongly on the cutoff radius R_C. For the SPC water model and with $R_{LJ} \sim 4$ Å, $R_C/L = 0.5$, $L \sim 20$ Å. This gives a value of $\langle\phi_{2,M}(0; R_C)\rangle$ of ca. 9 kcal/(mol·e). From the data of Figure 3 of Hummer et al.,[12] one finds that the simulated potential $\langle\phi_{2,M}(0; R_C)\rangle$ is ca. 9−10 kcal/(mole·e) for R_C near 10 Å (i.e., R_C near $L/2$), in agreement with the analytical estimate. Rick and Berne[18] as well have noticed that the solute potential calculated with tinfoil Ewald summation contains a large term, although this has only a slight influence on the structural properties of water.

Of course, a calculation based on the Ewald potential with the use of a cutoff sphere can be used only if R_C is less than half the cell edge, because sampling should not extend beyond the boundaries of the central cell. The limiting value of the potential with inclusion of the contents of the entire cubic cell can be calculated by evaluating the integral of eq 20, but replacing the integral over a concentric shell, $\int_{R_{LJ}}^{R_C} \pi r^2 dr$ with an integral over the volume of the box, $\int_0^L dx \int_0^L dy \int_0^L dz$, and excluding the volume of the LJ particle at the center (radius R_{LJ}).

Solving this integral, one obtains (always with the assumption of uniform distribution of molecular centers and molecular orientation)

$$\langle\phi_{2,M}(0; L) = \frac{2\pi\rho_w}{3}\sum_\alpha q_\alpha h_\alpha^2\left[1 - \frac{R_{LJ}^3}{L^3}\right] \quad (22)$$

In the limit of small radius of the LJ solute, this potential is equal to the surface potential $\phi_{outer}(0)$ of eq 7, but of opposite sign, and hence these two potentials cancel each other in the complete M-based tinfoil Ewald potential. Taking into account eqs 18a and 18b, one can conclude that the tinfoil Ewald M-based potential satisfies

$$\langle\phi^{tf}_{EW,M}(0; L)\rangle_{cub} \approx \langle\phi_{C,q}(0; R_C)\rangle = \langle\phi_{EW,q}(0; R_C)\rangle \quad (23)$$

Consider now the q-based potential in a high-temperature limit. In this limit the density for each atomic charge is uniform, except near the surface of the LJ solute. Because of electrical neutrality, the uniform density gives zero contribution to the integral of the tinfoil term $2\pi r^2/(3L^3)$, and only the surface charge distribution at the solute−solvent interface need be considered. Integration gives

$$\langle\phi_{2,q}(0; R_C)\rangle = 4\pi\rho_w \int_0^{R_C} \sum_\alpha Q_{inner}(r) \frac{2\pi r^2}{3L^3} r^2 dr = -\frac{8\pi^2\rho_w}{9}\frac{R_{LJ}^3}{L^3}\sum_\alpha q_\alpha h_\alpha^2 \quad (24)$$

Because only charge density at small values of r contributes, this term makes a small contribution to the q-based potential; for the SPC water model the value is ca. −0.6 kcal/(mol·e) for $(R_{LJ}/L) \sim 0.2$, $L \sim 20$ Å. Hence, the q-based potentials calculated with Ewald vacuum or tinfoil potentials are close, i.e.

$$\langle\phi^{tf}_{EW,q}(0; R_C)\rangle \approx \langle\phi_{EW,q}(0; R_C)\rangle \quad (25)$$

Combined with eq 22, this relation gives

$$\langle\phi^{tf}_{EW,M}(0; L)\rangle_{cub} \approx \langle\phi_{C,q}(0; R_C)\rangle = \langle\phi_{EW,q}(0; R_C)\rangle \approx \langle\phi^{tf}_{EW,q}(0;R_C)\rangle \quad (26)$$

Monte Carlo simulation results (Figure 3 of Hummer et al.[12]) for a large cutoff ($L/2 < R_C < L$) show convergence of the M-based potential $\langle\phi^{tf}_{EW,M}(0; R_C)\rangle$ to the q-based potential $\langle\phi^{tf}_{EW,q}(0;R_C)\rangle$, in agreement with the above analysis. The tinnfoil reaction potential cancels the outer surface potential of the polar liquid drop (see section 4). Therefore the q-based method, which ignores the outer surface potential, is insensitive to the tinnfoil conditions, while the M-based method, which reproduces the outer surface potential, becomes in the tinfoil case equal to the q-potential because the tinfoil reaction potential cancels out the potential of the cutoff surface.

The tinfoil boundary conditions add to the infinite spherical sample of cubic cells an instantly responding reaction field, which enhances the dipole−dipole correlation[7] and the periodicity of the simulated system. It can be seen that the tinfoil reaction field energy H^{tf}_{rf}, eq 17a, is actually equal to the reaction field energy of an isolated spherical sample of the same volume inserted in a conducting medium, while in actuality the central cell is surrounded by an infinite layer of replica cells. Thus, the Ewald sum with tinfoil boundary conditions effectively includes twice the interaction of the central cell with its surroundings.

6. Conclusion

The results of this paper resolve a controversy[3] about the appropriate cutoff method and the choice of molecular center for use in molecular simulations, and confirm that the intuitively obvious, and in practice more convenient, molecule-based cutoff is preferable when computing a charge density and related Coulomb potential inside a cavity, while significant artifacts arise with use of a charge-based cutoff, which violates the self-consistency of the statistical sampling of the configurations of the charged sites of the solvent molecules. This work also shows that artifacts arise under the best of circumstances as a result of the difficulty of representing the outer surface and taking into account its dipole density. The Coulomb potential at the center of a cavity inside a sample of simulated water is negative, ca. −10 kcal/(mole·e), due to preferential orientation of the water molecules at the surface of the cavity; an outer water−vacuum surface produces a potential of between +2 and +3 kcal/(mole·e), which in part cancels the former. This potential

affects the free energy of introducing a molecule having nonzero net charge inside the cavity by gradually increasing the magnitude of the atomic charges, but not the free energy of introducing in a similar manner a molecule having zero net charge. Also, the potential produces no net force on charged particles placed inside the cavity.

An important conclusion is that for simulations of infinite periodic systems, Ewald summation with vacuum boundary conditions is preferable over Ewald summation with tinfoil boundary conditions. This is based on the observation that the former most closely reproduces the use of M-based cutoff in simulations of finite systems. Also, the tinfoil conditions are seen to overestimate the interaction of the central cell with the surrounding medium and to enhance periodicity and polarization, which is inconsistent with applications to intrinsically aperiodic liquid systems. Inherent in the use of an infinite periodic system is the inability to capture the polarization of an outer surface and its effect on the potential.

7. Methods

MD simulations of an LJ "methane" molecule in SPC water solution have been done with periodic boundary conditions using a cubic box of edge 12 Å containing 454 water molecules, with (M-based) cutoff on nonbonded forces of 11.5 Å and Ewald summation (vacuum boundary conditions) at temperatures of 300 K (NTP ensemble, $P = 1$ bar), and 500 and 1000 K, (NTV ensemble with density $\sim$0.0333 Å^{-3}). Equilibrium MD trajectories of 250 ps were collected for calculation of charge densities, potentials, and dipole moment vector distributions. In MD simulations of a water droplet, the molecules were contained in a hydrophobic cavity with a wall at radius 21 Å exerting a r^{-6} repulsive potential on each water molecule's oxygen atom.[9,20] One uncharged molecule with LJ parameters equal to those of the SPC water oxygen atom was held at the center of the droplet. The droplet contained 995 SPC water molecules; simulations were done at 300 K, with (M-based) cutoff on nonbonded forces of 10 Å. All MD simulations have been done with the Sigma program.[9]

Acknowledgment. This work was supported by a grant from the National Center for Research Resources of the National Institutes of Health (RR08102).

References and Notes

(1) Allen, M. P.; Tildesley, D. J. *Computer simulation of liquids*; Oxford Press: New York, 1994.

(2) Aqvist, J.; Hansson, T. *J. Phys. Chem.* **1996**, *100*, 9512−9521.

(3) Aqvist, J.; Hansson, T. *J. Phys. Chem.* **1998**, *B 102*, 3837−3840.

(4) Ashbaugh, H. S.; Sakane, S.; Wood, R. H. *J. Phys. Chem.* **1998**, *B 102*, 3844−3845.

(5) Ashbaugh, H. S.; Wood, R. H. *J. Phys. Chem.* **1997**, *106*, 8135-8139.

(6) Belch, A.; Berkowitz, M. *Chem. Phys. Lett.* **1985**, *113*, 278−282.

(7) De Leeuw, S. W.; Perram, J. W.; Smith, E. R. *Proc. R. Soc. London* **1980**, *A 373*, 27−56.

(8) Hansen, J. P.; McDonald, I. R. *Theory of simple liquids*.; Academic Press: New York, 1986.

(9) Hermans, J.; Yun, R. H.; Leech, J.; Cavanaugh, D. Sigma documentation.; University of North Carolina: http://femto.med.unc.edu/SIGMA/, 1994.

(10) Hummer, G.; Pratt, L. R.; Garcia, A. E. *J. Phys. Chem.* **1995**, *99*, 14188−14194.

(11) Hummer, G.; Pratt, L. R.; Garcia, A. E. *J. Phys. Chem.* **1996**, *100*, 1206−1215.

(12) Hummer, G.; Pratt, L. R.; Garcia, A. E. *J. Phys. Chem.* **1997**, *B 101*, 3017−3020.

(13) Hummer, G.; Pratt, L. R.; Garcia, A. E.; Garde, S. *J. Phys. Chem.* **1998**, *B 102*, 3841−3843.

(14) Jayaram, B.; Fine, R.; Sharp, K.; Honig, B. *J. Phys. Chem.* **1989**, *93*, 4320−4327.

(15) Landau, L. D.; Lifshitz, E. M. Electrodynamics of continuous media. In *Course of theoretical physics* (Translated from the Russian); Pergamon Press: Oxford, 1988; Vol. 8.

(16) Leach, A. R. *Molecular Modeling. Principles and Applications*; Longman: Singapore, 1997.

(17) Motakabbir, K. A.; Berkowitz, M. L. *Chem. Phys. Lett.* **1991**, *176*, 61−66.

(18) Rick, S. W.; Berne, B. J. *J. Am. Chem. Soc.* **1994**, *116*, 3949−3954.

(19) Taylor, R. S.; Dang, L. X.; Garrett, B. C. *J. Phys. Chem.* **1996**, *100*, 11720−11725.

(20) Wang, L.; Hermans, J. *Mol. Simul.* **1996**, *17*, 67−74.

(21) Wilson, M. A.; Pohorille, A.; Pratt, L. R. *J. Chem. Phys.* **1989**, *90*, 5211−5214.